

# A non-canonical role for the *C. elegans* dosage compensation complex in growth and metabolic regulation downstream of TOR complex 2

Christopher M. Webster<sup>1,2</sup>, Lianfeng Wu<sup>1,2</sup>, Denzil Douglas<sup>1,2</sup> and Alexander A. Soukas<sup>1,2,\*</sup>

## SUMMARY

The target of rapamycin complex 2 (TORC2) pathway is evolutionarily conserved and regulates cellular energetics, growth and metabolism. Loss of function of the essential TORC2 subunit Rictor (RICT-1) in *Caenorhabditis elegans* results in slow developmental rate, reduced brood size, small body size, increased fat mass and truncated lifespan. We performed a *rict-1* suppressor RNAi screen of genes encoding proteins that possess the phosphorylation sequence of the AGC family kinase SGK, a key downstream effector of TORC2. Only RNAi to *dpy-21* suppressed *rict-1* slow developmental rate. DPY-21 functions canonically in the ten-protein dosage compensation complex (DCC) to downregulate the expression of X-linked genes only in hermaphroditic worms. However, we find that *dpy-21* functions outside of its canonical role, as RNAi to *dpy-21* suppresses TORC2 mutant developmental delay in *rict-1* males and hermaphrodites. RNAi to *dpy-21* normalized brood size and fat storage phenotypes in *rict-1* mutants, but failed to restore normal body size and normal lifespan. Further dissection of the DCC via RNAi revealed that other complex members phenocopy the *dpy-21* suppression of *rict-1*, as did RNAi to the DCC effectors *set-1* and *set-4*, which methylate histone 4 on lysine 20 (H4K20). TORC2/*rict-1* animals show dysregulation of H4K20 mono- and tri-methyl silencing epigenetic marks, evidence of altered DCC, SET-1 and SET-4 activity. DPY-21 protein physically interacts with the protein kinase SGK-1, suggesting that TORC2 directly regulates the DCC. Together, the data suggest non-canonical, negative regulation of growth and reproduction by DPY-21 via DCC, SET-1 and SET-4 downstream of TORC2 in *C. elegans*.

**KEY WORDS:** Target of rapamycin (TOR), TOR complex 2 (TORC2), Dosage compensation complex (DCC), Rictor, Metabolism, Growth, Aging, *C. elegans*, Epigenetics, *dpy-21*

## INTRODUCTION

The target of rapamycin (TOR) kinase regulates metabolism, development, growth and lifespan by its action in two distinct complexes: TOR complex 1 and TOR complex 2 (Bhaskar and Hay, 2007; Alessi et al., 2009; Jones et al., 2009; Soukas et al., 2009; Lamming et al., 2012). In *C. elegans*, loss-of-function mutations in the gene encoding the essential TOR complex 2 (TORC2) member RICT-1 leads to small worms with delayed larval development, reduced brood size and shortened lifespan with seemingly inappropriately increased fat stores (Soukas et al., 2009). These phenotypes, with the exception of increased body fat, associated with mutation of TORC2 can be phenocopied by loss of function of the downstream serum and glucocorticoid-induced kinase (SGK-1), a protein kinase A, protein kinase G, protein kinase C (AGC) family kinase.

In *C. elegans*, gain-of-function mutations in *sgk-1* partially suppress the high fat and small body size phenotypes of the TORC2 mutant *rict-1* (Jones et al., 2009). Similarly, gain-of-function mutations in Ypk2, the yeast ortholog of Sgk, suppress the lethality of *Saccharomyces cerevisiae* TORC2 mutations through effects on ceramide metabolism (Kamada et al., 2005; Aronova et al., 2008). Mammalian TORC2 (mTORC2) also phosphorylates and activates

Sgk (García-Martínez and Alessi, 2008), though key differences between mammals and lower eukaryotes exist. In knockout mice, it is the protein kinase Akt that mediates many of the metabolic effects of mTORC2 (Bhaskar and Hay, 2007; Hagiwara et al., 2012; Lamming et al., 2012; Yuan et al., 2012). Whereas defects in glucose metabolism in mTORC2 knockout mice are the result of defective Akt signaling through FoxO (Hagiwara et al., 2012; Yuan et al., 2012), in *C. elegans*, the growth, reproductive and lifespan-shortening phenotypes of TORC2 mutants do not depend upon AKT signaling through FoxO (Jones et al., 2009; Soukas et al., 2009). Still, certain aspects of mammalian metabolic regulation by TORC2 cannot be fully explained by loss of Akt activation, indicating additional, unelucidated outputs of TORC2 signaling (Yuan et al., 2012).

In *C. elegans*, understanding of the genetics of the TORC2 pathway remains incomplete. Although the lifespan of *C. elegans* TORC2 mutants is shortened under standard laboratory conditions, inactivation of TORC2 by RNAi leads to lifespan extension in a manner dependent upon the Nrf ortholog SKN-1 (Hertweck et al., 2004; Soukas et al., 2009; Robida-Stubbs et al., 2012). Other phenotypes of TORC2 mutants are not suppressed by loss of *skn-1* (Soukas et al., 2009). Thus, mechanistic knowledge of TORC2 and SGK-1 signaling that modulates metabolism, growth and reproduction is incomplete.

In yeast, TOR has been tied to alterations in chromatin structure. TORC1 mutations in *S. pombe* lead to dysregulated chromatin structure (Rohde and Cardenas, 2003; Tsang et al., 2003). Alternatively, yeast TORC2 mutants demonstrated altered heterochromatin structure with upregulation of repeated elements and subtelomeric genes resembling mutations in histone deacetylase

<sup>1</sup>Center for Human Genetic Research and Diabetes Unit, Department of Medicine, Massachusetts General Hospital, Boston, MA 02114, USA. <sup>2</sup>Department of Medicine, Harvard Medical School, Boston, MA 02115, USA.

\* Author for correspondence (asoukas@chgr.mgh.harvard.edu)

or RSC chromatin remodeling complex members (Schonbrun et al., 2009). In *C. elegans*, however, studies have not yet illuminated the role of epigenetic regulation in TOR biology.

*C. elegans* exists as either a male (XO) or a hermaphrodite (a self-fertilizing XX female with larval stage spermatogenesis). Much like humans and other animals, *C. elegans* males have one X chromosome and thus have half of the X chromosomal gene dosage of female or hermaphroditic animals. X chromosomal dosage compensation (DC) has evolved in order to equalize the expression of the X-linked genes between males and females. The mechanisms by which DC occurs varies greatly between species: mammals transcriptionally mute expression of one of the two female X chromosomes (Lyon, 1961), flies double the expression of the single male X chromosome (Gelbart and Kuroda, 2009) and the *C. elegans* hermaphrodite downregulates gene expression from both X chromosomes by 50% (Meyer and Casson, 1986). This X chromosomal regulation is orchestrated through the dosage compensation complex (DCC).

The *C. elegans* DCC binds to both X chromosomes in the hermaphrodite to downregulate gene expression by half. The DCC is highly specialized and consists of a core condensin 1-like complex composed of three chromosome-associated polypeptides (DPY-26, DPY-28 and CAPG-1) and two structural maintenance proteins (MIX-1 and DPY-27) involved in chromosomal structure and segregation. Other associated members of the DCC include the SDC-1, SDC-2, SDC-3, DPY-30 and DPY-21, which, through SDC-2, SDC-3 and DPY-30, allow for the DCC to be recruited specifically to the X chromosome in the hermaphrodite. The mechanism of DCC downregulation of X chromosomal genes remains elusive; however, two recent investigations suggest that the DCC stimulates formation of the repressive epigenetic mark histone 4, lysine 20 monomethyl (H4K20me1) (Vielle et al., 2012; Wells et al., 2012). Further, the DCC is required for the enrichment of H4K20me1 on the X chromosome, as loss of *dpy-21* reduces H4K20me1 (Vielle et al., 2012). The histone 4 lysine 20 (H4K20) monomethyltransferase SET-1 and di/trimethyltransferase SET-4, as well as the histone deacetylase SIR-2.1, play key roles in regulating the methylation state and acetylation state of histone H4 on the X chromosome downstream of the DCC (Wells et al., 2012).

In the present study, we identified DCC member *dpy-21* through a reverse RNAi genetic screen for suppressors of the slow growth phenotype of *riect-1* animals. *dpy-21* inactivation suppresses multiple TORC2/*riect-1* pleiotropies, restoring a near-normal brood size and reducing elevated fat mass to normal levels. Further investigation revealed that knockdown of other members of the DCC could also suppress *riect-1* phenotypes, suggesting that the DCC acts downstream of TORC2/*riect-1* to negatively regulate growth, reproduction and metabolism. Knockdown of *dpy-21* resulted in a faster larval development for both hermaphrodites and male worms alike, implying a non-canonical mechanism of DCC functionality to suppress gene expression independent of gender. Genomic inactivation of *dpy-21* negatively influenced the lifespan of *riect-1* animals, suggesting that loss of *dpy-21* is beneficial for larval development but results in detrimental effects on longevity in adult worms. We uncovered the histone 4 lysine 20 (H4K20) monomethyltransferase SET-1 and di/trimethyltransferase SET-4 as the major effectors of DCC functionality downstream of TORC2. Interestingly, *riect-1* mutant animals are depleted of H4K20 monomethyl marks (H4K20me1 and H4K20me3), which is suppressed by abrogation of DCC activity. The data suggest a major role for epigenetic regulation in mediating TORC2 phenotypes and that a complex balance of H4K20 methylation is necessary for

regulation of normal development, growth and metabolism. Finally, we find that DPY-21 protein physically associates with SGK-1, a major downstream kinase in the TORC2 pathway, suggesting that TORC2 directly regulates the DCC. The current work ties TORC2 signaling to epigenetic gene regulatory mechanisms, and invokes a new role for the DCC in development and metabolism through autosomal gene regulation. We propose that the DCC and DPY-21 are novel downstream negative regulators of the TORC2/SGK-1 pathway.

## MATERIALS AND METHODS

### Strains and maintenance

*C. elegans* animals were grown and maintained on Nematode Growth Media (NGM) seeded with *Escherichia coli* OP50 as previously described (Soukas et al., 2009). The wild-type strain was N2 Bristol. The following *C. elegans* mutant strains were used: MGH1 *riect-1(mg451)*, MGH2 *riect-1(mg450)*, MGH26 *riect-1(mg451);sgk-1(mg455)*, MGH35 *sinh-1(mg452)*, CB428 *dpy-21(e428)*, MGH229 *dpy-21(e428);riect-1(mg451)* and MGH12 *mgIs60[SGK-1::GFP pRF4]*.

Synchronization of animals was performed through egg preparation of a well-fed, gravid adult population of worms. Adult animals were collected into M9 media and centrifuged at 4000 rpm (3300 g) for 30 seconds. The worm pellet was resuspended in a solution of 1.3% bleach and 250 mM NaOH, and agitated until worm corpses dissolved or 5 minutes had elapsed, whichever occurred first. Eggs were quickly centrifuged at 4000 rpm for 30 seconds and the supernatant removed. Eggs were washed with sterile M9 five times. Eggs were resuspended in 6 ml M9 and allowed to hatch and synchronize to L1 larvae for 18 hours at 20°C with gentle rotation.

### RNA interference (RNAi)

RNAi clones were isolated from a genome-wide *E. coli* RNAi library, sequence verified, and fed to animals as described (Kamath and Ahringer, 2003). RNAi feeding plates (6 cm) were prepared using a standard NGM recipe with 5 mM isopropyl-β-D-thiogalactopyranoside and 200 μg/ml carbenicillin. RNAi clones were grown for 15 hours in Luria Broth (LB) containing 200 μg/ml carbenicillin with shaking at 37°C. The stationary phase culture was then collected, concentrated through centrifugation, the supernatant discarded and the pellet resuspended in LB to 10% of the original culture volume; 300 μl of each RNAi clone concentrate was added to RNAi plates and allowed to dry no more than 48 hours prior to adding the worm embryos or animals.

### Developmental timing

Developmental timing analysis was conducted on synchronized L1 animals prepared as above. Synchronous animals were dropped onto RNAi plates containing an empty vector RNAi control or a sequence-verified target RNAi in *E. coli* HT115 and grown at 15°C. Time to adulthood was measured from the time when synchronized L1 animals were first exposed to food until the time at which the animal reached adulthood. Hermaphrodite animals were scored for their transition into adulthood by appearance of the vulvar slit. Male adulthood was determined by ray and fan formation (Nguyen et al., 1999). Two to three biological replicates were carried out for each condition examined and data are displayed in the supplementary material as indicated in the text.

### Brood size determination

Synchronous L1 larvae were dropped onto RNAi plates containing appropriate RNAi *E. coli* bacteria. After growing to young adulthood, single animals were transferred to new NGM plates containing fresh bacteria containing the same RNAi clone each day for 5 days ( $n=10$  per group). Progeny from parents were counted and summed from each of the five transfer plates to determine brood size.

### Body fat measurement

Body fat mass was measured as previously described (Pino et al., 2013). All analyses were performed on identically staged young adult worms, which were washed off of RNAi plates, fixed in 40% isopropanol for 3 minutes, and stained in 40% isopropanol containing 3 μg/ml Nile Red.

Worms were washed with PBS with 0.01% Triton X-100, mounted on agarose pads, and fluorescently imaged using GFP/FITC filters. Body fat mass was scored by fluorescence detection of the Nile Red-stained *C. elegans* lipid droplets using MetaMorph software and expressed as the mean of at least 25 animals per group.

#### Body size determination

Body size of *C. elegans* mutants was determined as the maximal, longitudinal, cross-sectional area and measured as previously described (Soukas et al., 2009). Synchronous L1 larvae were exposed to RNAi plates containing the appropriate RNAi strain. Animals were processed as above for body fat measurement, imaged by brightfield microscopy, and body area calculated by MetaMorph software for a minimum of 25 animals per group.

#### Longevity assay

Synchronous L1 animals were placed on RNAi plates seeded with the appropriate RNAi clone, either empty vector or *dpy-21* RNAi. As day 1 adults, 30 animals per genotype were transferred in quadruplicate (120 total) to fresh RNAi plates with the corresponding RNAi supplemented with 10–50  $\mu$ M 5-fluorodeoxyuridine (FUDR) solution to suppress progeny production. Three independent assays were carried out with concordant results. Live, dead and censored worms were calculated daily in the worm populations by scoring movement with gentle prodding when necessary. Data were analyzed and statistics performed through OASIS (<http://sbi.postech.ac.kr/oasis/surv/>). A Kaplan–Meier estimator and a log cumulative hazard plot provided by OASIS were used to estimate individual survival and mortality over the lifespan of the worms. A non-parametric Mantel–Cox log-rank test was used for comparison of different survival functions.

#### Isolation of the *sinh-1(mg452)* mutant

The *mg452* mutant was obtained from an F2 forward genetic screen that has been previously described (Soukas et al., 2009). Individual isolates were backcrossed to N2 Bristol and positionally cloned based on polymorphisms between N2 and the multiply polymorphic *C. elegans* strain CB4586.

#### Western blot analysis

Five thousand synchronous mid-L4 stage animals were collected for each genotype and knocked down. Collected worms were washed three times in M9 media and snap frozen in liquid nitrogen. Worms were thawed on ice by adding two pellet volumes of 1% SDS, 50 mM Tris, pH 7.4, and 100 mM NaCl, heated to 80°C on a dry heat block for 5 minutes, and sonicated in a BioRuptor XL for 10 minutes on maximum intensity (30 second pulses with 30 seconds rest between pulses) to obtain lysates. Lysates were cleared by centrifugation at 21,000 *g* for 15 minutes. Sixty micrograms of total worm protein was electrophoresed by SDS-PAGE, and transferred to nitrocellulose membrane. Even transfer was confirmed by Ponceau S staining. Membranes were blocked with TBST (TBS + 0.1% Tween20) containing 5% nonfat milk, washed twice with TBST, and blotted overnight at 4°C with anti-H4K20me1 (Abcam, ab9051) rabbit polyclonal antibody at 1:2000, anti-H4K20me3 (Abcam, ab78517) mouse monoclonal antibody at 1:500, or total histone H4 (Abcam, ab10158) rabbit polyclonal antibody at 1:1000 in TBST and 5% BSA. Anti-rabbit HRP secondary antibody (Thermo Pierce) was used at 1:10,000 (H4K20me1 and total histone H4) or anti-mouse HRP secondary antibody (Thermo Pierce) at 1:10,000 (H4K20me3), all in TBST at room temperature for 2 hours. Thermo SuperSignal West Pico Chemiluminescent Substrate Kit was used for detection.

#### DPY-21 pull down assay

The C-terminus of the *C. elegans dpy-21* gene was cloned into the pGEX-KG vector under the control of the *tac* promoter. The 1626 base pair fragment was amplified from wild-type (WT) worm cDNA using the following primers: PF, TACGTCGACTCGAGCAGTTGATGTCG-AGGAAG; PR, ACCAAGCTTCTATTTCAGTTGATTCACGCACCTG. The fragment and vector was digested with *Hind*III and *Sal*I and individually gel purified. The fragments were ligated to produce pGST-DPY-21(920-1461). GST-DPY-21(920-1461) was expressed in *E. coli* BL21(DE3)plysS from pGEX-KG plasmids and purified with Pierce GST Spin Purification Kit (Thermo Scientific, Prod# 16106). Five micrograms

purified GST and GST-DPY-21(920-1461) proteins were re-immobilized with pre-equilibrated 20  $\mu$ l GST beads in lysis buffer.

Three milliliters of packed, mixed-stage SGK-1::GFP transgenic worms were collected and washed three times in M9 buffer and stored at –80°C. Worms were freeze ground and lysed in lysis buffer [1  $\times$  PBS, 1 mM EDTA, 0.5% NP-40, 50 mM  $\beta$ -glycerophosphate, 0.1 mM NaVO<sub>4</sub>, 50 mM NaF and protease inhibitor cocktail (EDTA-free, Roche)]. The worm extract was further lysed twice through French Pressure cell (Thermo Scientific) and centrifuged for 30 minutes at 38,000 rpm (178,000 *g*) at 4°C in a Beckman Ti-41 rotor. The supernatant was filtered through a 0.45  $\mu$ m filter and protein concentration determined with Pierce BCA Protein Assay Kit (Thermo Scientific) before the pull down assay. Three hundred milliliters of 5  $\mu$ g/ml SGK-1::GFP lysate was incubated with the immobilized beads at 4°C for 1.5 hours. After washing beads three times with lysis buffer, samples were analyzed by western blot using rat anti-GFP antibody (JFP-J5, Riken, 1:2000).

## RESULTS

### *dpy-21* RNAi suppresses growth delay, reproductive defects and elevated fat mass of the *C. elegans* TORC2 mutant *rict-1*

Our previous work shows that mutations in *rict-1* (ortholog of human Rictor), a critical subunit of the heteromeric kinase TOR complex 2 (TORC2) in *C. elegans*, lead to developmental delay (Soukas et al., 2009). In order to identify genes acting downstream of TORC2/SGK-1 regulating the essential process of development, we performed a reverse genetic RNA interference (RNAi) screen to genes encoding proteins that contain the potential target phosphorylation sequence for SGK-1 (RXXXS/T-p) (Bodenmiller et al., 2008).

RNAi to only one of these genes, *dpy-21*, a member of the DCC (Meyer, 2005), significantly suppressed the developmental delay evident in *rict-1* mutants in multiple replicate experiments. In order to quantify the suppression of *rict-1* developmental delay, we studied the developmental timing profile of both wild type and *rict-1* mutants exposed to *dpy-21* RNAi. We measured the time from the L1 larval stage to development of the mature vulva (indicative of the young adult stage), and found that *dpy-21* RNAi significantly shortened the average time to adulthood of *rict-1* mutants (Fig. 1A; supplementary material Table S1). We were surprised to see that *dpy-21* RNAi also significantly, albeit to a much lesser extent, shortened developmental timing in wild-type animals (Fig. 1A; supplementary material Table S1). Data from triplicate analyses were consistent with these findings (supplementary material Table S1). This indicates that reduction in function of *dpy-21* accelerates development and does so downstream of TORC2.

We next measured other pleiotropies of *rict-1* mutants when exposed to *dpy-21* RNAi. *rict-1* mutants at young adulthood show a 30–100% increase in fat mass as assessed by fixation-based lipid staining or quantitative lipid biochemistry (Fig. 1B) (Soukas et al., 2009). RNAi to *dpy-21* fully rescued the increased fat mass of *rict-1* mutant animals to a level equivalent to that of wild-type animals (Fig. 1B). *dpy-21* knockdown also reduced the fat mass of wild-type animals; however, the effect was much less powerful than in *rict-1* mutants.

*rict-1* mutants have a brood size that is ~40% of wild-type animals, and deliver that brood over a much longer time period than do wild type (Fig. 1C,D; supplementary material Table S2) (Soukas et al., 2009). When treated with RNAi to *dpy-21*, brood size was returned nearly to normal for *rict-1* mutants, and the progeny was delivered over a much shorter timespan than the control mutant animals (Fig. 1C,D). This effect was consistent between triplicate analyses of *rict-1* brood with *dpy-21* RNAi (supplementary material Table S2). *dpy-21* RNAi had no effect on the brood size of wild-type animals.

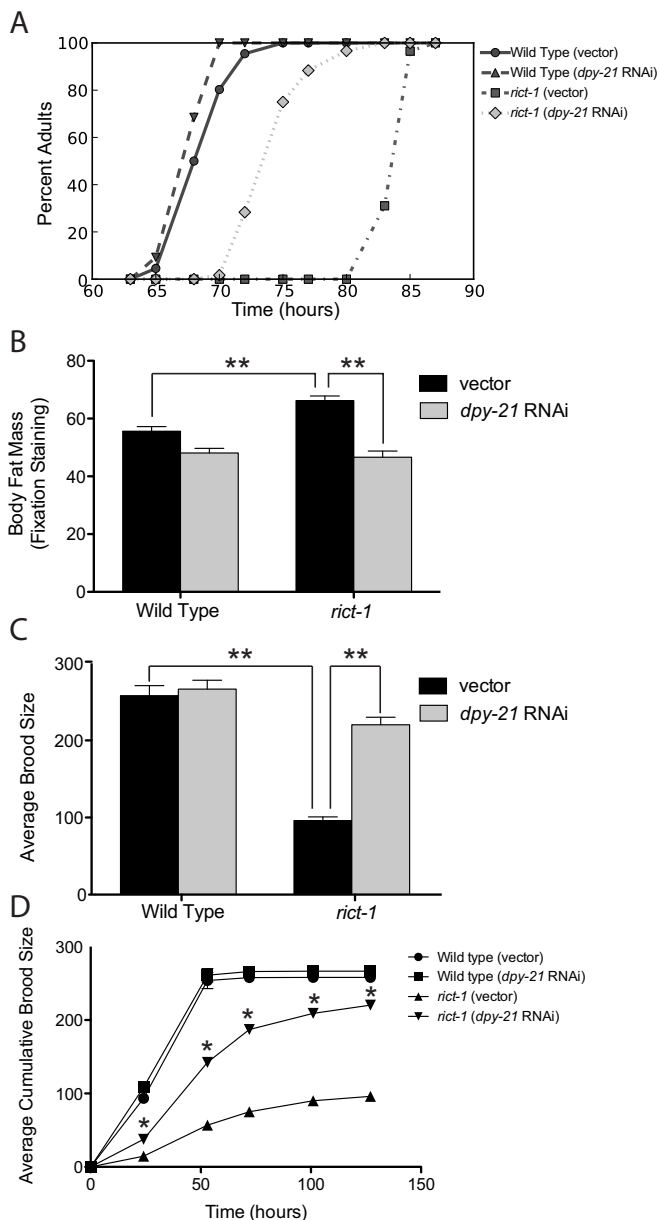


**Fig. 1. Developmental delay, elevated fat mass and low brood size of the TORC2 mutant *rict-1* are suppressed by RNAi of *dpy-21*.**

(A) Developmental rate of *rict-1* mutants is accelerated by 10 hours by *dpy-21* RNAi. Curves are significantly different from each other by log-rank test, Bonferroni corrected, at  $P < 0.01$  [wild type(vector) versus wild type(*dpy-21* RNAi)] or  $P < 0.0001$  (all other comparisons). (B) Body fat mass, as assessed by fixation-based Nile Red staining (Pino et al., 2013), was elevated in *rict-1* mutants, reduced in wild-type animals by *dpy-21* RNAi and reduced to wild-type levels by *dpy-21* RNAi in *rict-1* ( $n \geq 25$  per group). (C) *dpy-21* RNAi in *rict-1* animals increased total brood size per animal to near wild-type levels ( $n = 10$  per group). (D) *rict-1* brood delivery over time. *dpy-21* RNAi increased *rict-1* brood delivery rate ( $n = 10$  per group). \* $P < 0.01$ , \*\* $P < 0.0001$  by two-way ANOVA. Error bars represent s.e.m.

We next analyzed *dpy-21* loss-of-function mutants. Unlike RNAi, nonsense mutations of *dpy-21* lead to dramatically slowed developmental rate and reduced brood size, and to further delayed development and reduced brood size in *dpy-21*;*rict-1* double mutants (supplementary material Fig. S1A-C). This suggested that partial reduction of DPY-21 function or a spatiotemporal loss of

function that was not recapitulated by nonsense mutation in *dpy-21* was needed to suppress *rict-1* mutant phenotypes. Although body fat mass was decreased in *dpy-21*;*rict-1* double mutants (supplementary material Fig. S1D), we believe this to be a consequence of the poor fitness of the double mutant animal, as body size in *dpy-21* and *dpy-21*;*rict-1* double mutants was substantially decreased (supplementary material Fig. S1E). We confirmed that *dpy-21* mRNA was efficiently knocked down ( $88.8 \pm 9.7\%$ ,  $P < 0.02$ ) by *dpy-21* RNAi (data not shown). Thus, RNAi was used for all subsequent analyses.

### ***dpy-21* RNAi demonstrates negative effects on *rict-1* lifespan and body size**

In spite of *dpy-21* RNAi suppressing multiple *rict-1* mutant phenotypes, we noted negative effects when lifespan and body size were examined. *dpy-21* RNAi significantly shortened the lifespan of *rict-1* mutants from an average of  $14.1 \pm 0.28$  days (mean  $\pm$  s.e.m.) (vector RNAi) to  $9.36 \pm 0.37$  days (*dpy-21* RNAi) (Fig. 2A; triplicate analysis in supplementary material Table S3) at  $20^\circ\text{C}$ . *dpy-21* RNAi also shortened lifespan in wild-type animals to an equivalent extent, suggesting that, unlike for growth rate, fat mass and brood size, *dpy-21* does not act in the same pathway as *rict-1* when modulating lifespan. In a similar fashion, *rict-1* mutants, which are normally 75% of the area of wild-type worms at a similar developmental stage, when treated with *dpy-21* RNAi showed a further 15% decrease in body size (Fig. 2B; supplementary material Fig. S2A). Thus, RNAi to *dpy-21* seems to positively affect larval growth rate, reduce fat mass and boost brood size at the expense of shortened lifespan and reduced overall body size.

### ***dpy-21* regulates growth rate in a TORC2-specific pathway downstream of *sgk-1***

In order to establish that *dpy-21* regulates growth specifically in the TORC2 pathway, we returned to the forward genetic screen in which we had previously isolated two loss-of-function alleles in *rict-1* (*mg450* and *mg451*) and two loss-of-function mutations in *sgk-1* (*mg455* and *mg456*) that phenocopy *rict-1* (Soukas et al., 2009). In this screen, we had isolated an additional mutant with slow growth and small body size that did not contain mutations in *sgk-1* or *rict-1* and mapped to LG II, albeit closer to the centromere than *rict-1*. Using the polymorphic strain CB4856 we refined the map location of this mutant, *mg452*, to a region containing another well-described essential subunit of TORC2, *sinh-1*, the *C. elegans* ortholog of mSin1 (Mapkap1 – Mouse Genome Informatics) (Fig. 3A) (Hansen et al., 2005). *mg452* contains an early stop mutation in the second to the last coding exon of *sinh-1*, predicted to truncate 139 of the total 642 amino acids from the C-terminus of SINH-1 (Fig. 3B).

We reasoned that if RNAi of *dpy-21* was acting to suppress *rict-1* phenotypes through activity in the TORC2 pathway, it should also suppress *sinh-1* mutant growth delay. Similar to *rict-1* mutants, *sinh-1*(*mg452*) mutants show a pronounced delay in reaching adulthood (Fig. 3C). RNAi of *dpy-21* in *sinh-1*(*mg452*) mutants led to suppression of growth delay (Fig. 3C; duplicate analysis in supplementary material Table S4).

TORC2 acts in a genetic pathway with *sgk-1* regulating growth rate, body size, reproduction, lifespan and fat mass (Jones et al., 2009; Soukas et al., 2009). *sgk-1* loss-of-function mutants show a similar developmental delay to *rict-1* animals (Fig. 3D), so we investigated whether *dpy-21* RNAi acted in a manner dependent upon SGK-1 or whether DPY-21 acts downstream of SGK-1. As *dpy-21* suppressed *rict-1*;*sgk-1* mutant growth delay, we reasoned

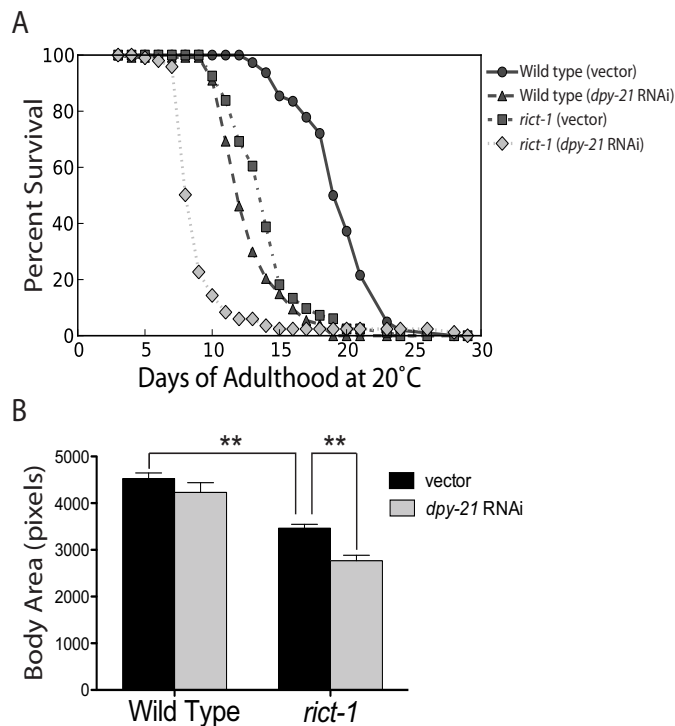


**Fig. 2. *dpy-21* RNAi produces negative effects on *rict-1* lifespan and body size.** (A) Lifespan of both wild-type and *rict-1* mutant animals is shortened by *dpy-21* RNAi. All curves are significantly different from each other by log-rank test, Bonferroni corrected, at  $P < 0.01$  for wild type (*dpy-21* RNAi) versus *rict-1* (vector), or  $P < 0.0001$  for all other comparisons. (B) Body area was significantly lower in *rict-1* mutants than in wild-type animals and was further reduced by *dpy-21* RNAi.  $**P < 0.0001$  by two-way ANOVA. Error bars represent s.e.m.

that DPY-21 was acting downstream of TORC2 and SGK-1 to regulate growth (Fig. 3D; duplicate analysis in supplementary material Table S4).

### Reduced function of the DCC by RNAi suppresses *rict-1* phenotypes

In *C. elegans*, DPY-21 acts as a member of the DCC. The DCC is responsible for binding to X chromosomes in somatic cells of hermaphrodite (XX) animals, thereby enacting changes that reduce X-linked gene expression by half (Meyer, 2005). Although the DCC functions canonically in hermaphrodite animals, it remains unknown how the specific DCC components interact with or affect other condensin complexes and cellular processes in the cell. In order to test whether *dpy-21* was functioning to suppress growth delay and reproductive defects in *rict-1* mutants through its role in the DCC, we inactivated six of the nine additional members of the DCC by RNAi in *rict-1* mutants. These data indicated that all six of these RNAi either suppressed growth delay or low brood size in *rict-1* mutants (Fig. 4). RNAi of the core DC component *dpy-27* (Chuang et al., 1994) had the strongest suppressive effect on *rict-1* developmental delay (Fig. 4A; supplementary material Table S5), followed by *dpy-30*, *sdc-1*, *sdc-2* and *capg-1* (Fig. 4C-F; supplementary material Table S5). Triplicate analyses showed consistent results (supplementary material Table S5).

Although RNAi of *sdc-2* and *dpy-28* had only minor effects on *rict-1* developmental rate (Fig. 4B,E; supplementary material Table S5), both RNAi significantly increased both the total brood size of

*rict-1* animals (Fig. 4G,H). RNAi to both *dpy-28* and *sdc-2* reduced the number of live progeny per animal for wild type, but had an exact opposite effect on *rict-1* mutants.

RNAi to *dpy-21* suppressed the elevated fat mass of *rict-1* mutants, so we determined next what effect knockdown of other DCC component genes had on fat mass. Much like *dpy-21*, RNAi to *dpy-27*, *dpy-28*, *dpy-30*, *sdc-1*, *sdc-2* and *capg-1* all reduced fat mass of *rict-1* mutants and had little effect in wild-type animals (Fig. 4). Further supporting the idea that knockdown of the DCC does not suppress the small body size pleiotropy of *rict-1* mutants, we saw no change or further decrease in body size with knockdown of DCC genes (supplementary material Fig. S2B).

### *dpy-21* RNAi suppresses male *rict-1* developmental delay, indicating a non-canonical role for the DCC in somatic gene regulation

The major reported role for the DCC is the reduction in X chromosomal gene expression in hermaphrodites. Given that male *C. elegans* carry a genotype of XO, the DCC does not perform X chromosomal dosage compensation in males. If RNAi to *dpy-21* was suppressing *rict-1* phenotypes by its canonical role in X chromosomal gene dosage, *rict-1* male growth delay should not be suppressed. We noted reproducible suppression of *rict-1* male growth delay by *dpy-21* RNAi, albeit to a lesser extent than in hermaphrodites (Fig. 5; supplementary material Table S6). Results were qualitatively similar in triplicate repeat experiments (supplementary material Table S6).

### RNAi of the DCC-regulated H4K20 monomethyltransferase *set-1* and di/trimethyltransferase *set-4* suppresses *rict-1* developmental delay and elevated fat mass

In embryos, the DCC controls methylation of histone H4 at lysine 20 (H4K20) such that in states of increased DCC activity, increased SET-1 activity leads to higher H4K20 monomethylation (H4K20me1) (Vielle et al., 2012). SET-4 activity, which di- and trimethylates H4K20, is correspondingly decreased during embryonic dosage compensation (Vielle et al., 2012), but SET-4 has been reported to mediate some of the effects of the DCC (Wells et al., 2012). H4K20me1 likely contributes to the chromosomal condensation (Nishioka et al., 2002; Rice et al., 2002), restricting expression of X chromosomal genes during dosage compensation. The role of H4K20me1 and H4K20me3 and their connection to the DCC post-embryonically has not been well established.

We hypothesized that altered gene expression as a consequence of modulations in chromosome condensation might be responsible for *rict-1* mutant developmental delay, decreased brood size and increased fat mass phenotypes. Given that H4K20me1 is responsible for mediating effects downstream of the DCC, we inactivated *set-1* in *rict-1* mutants by RNAi. *set-1* RNAi strongly suppressed developmental delay of *rict-1* mutants (Fig. 6A; supplementary material Table S7). Further, RNAi to *set-4* also potentially suppressed *rict-1* developmental delay (Fig. 6B; supplementary material Table S7). Triplicate analyses of *set-1* and *set-4* RNAi were consistent (supplementary material Table S7). *sir-2.1*, which has been reported to act to deacetylate lysine 16 of H4 (H4K16Ac) downstream of the DCC (Wells et al., 2012), also modestly suppressed developmental delay in *rict-1* mutants (Fig. 6C; supplementary material Table S7).

The elevated fat mass evident in *rict-1* mutants was reduced significantly by RNAi to *set-1* and *set-4* (Fig. 6D). Much like knockdown of *dpy-21*, RNAi to *set-1* and *set-4* did not suppress the

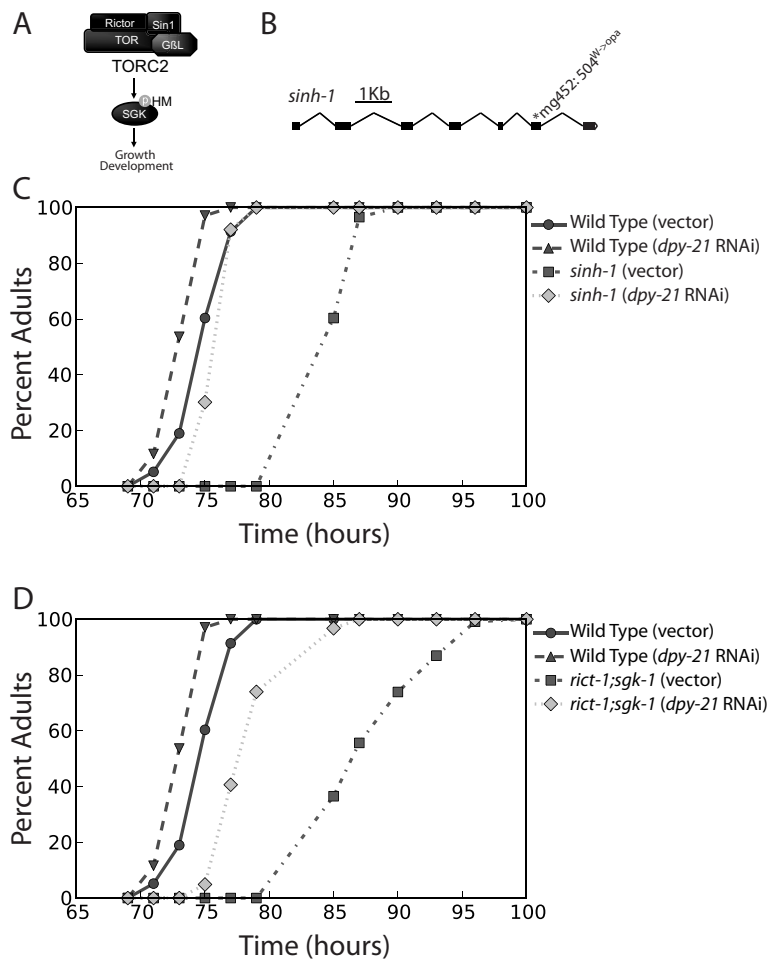


**Fig. 3. *dpy-21* RNAi suppresses growth delay in the TORC2 mutant *sinh-1* and acts downstream of the TORC2 pathway effector *sgk-1*.** (A) Schematic of current knowledge of *C. elegans* TORC2 signaling. (B) Schematic of the *C. elegans* Sin1 ortholog *sinh-1* genomic locus. Asterisk denotes the identified mutant *mg452*, which harbors an early stop mutation. (C) Developmental rate in the TORC2 subunit *sinh-1(mg452)* mutant, which is dramatically slowed relative to wild type, is accelerated to near wild-type levels by RNAi to *dpy-21*.  $P < 0.0001$  by log-rank test, Bonferroni corrected, for all comparisons except wild type(vector) versus wild type(*dpy-21* RNAi) ( $P < 0.01$ ). (D) Developmental rate in *rict-1;sgk-1* double mutants are also accelerated by *dpy-21* RNAi, indicating that *dpy-21* acts downstream of *sgk-1* to regulate development in the TORC2 pathway.  $P < 0.0001$  by log-rank test, Bonferroni corrected, for all comparisons except wild type(vector) versus wild type(*dpy-21* RNAi) ( $P < 0.01$ ).

small body size or shortened lifespan of *rict-1* mutants (Fig. 6E,F; supplementary material Table S8). This is further evidence that these H4K20 methyltransferases act as effectors of the DCC in the TORC2 pathway.

#### H4K20me1 and H4K20me3 marks are reduced in *rict-1* mutants and are reversed by RNAi to *dpy-21*

Although RNAi to the DCC component genes *set-1* and *set-4* can suppress TORC2 mutant phenotypes, it was not clear whether DCC, SET-1 and SET-4 activity are altered in TORC2 mutants, and whether this could be responsible for mutant phenotypes. The full extent of how epigenetic modifications affect biological phenotypes is not known; however, in yeast, loss of TOR signaling has been suggested to increase nucleolar condensation (Tsang et al., 2003). Thus, we next sought to determine whether TORC2/*rict-1* mutants have altered H4K20me1 or H4K20me3 marks. Despite our hypothesis that increased DCC activity in *rict-1* mutants would be positively correlated with H4K20me1 and H4K20me3, we found both marks to be decreased overall in *rict-1* mutants (Fig. 7A-D). This suggests that the DCC, at the post-embryonic developmental stage studied, is negatively correlated with SET-1 and SET-4 activity. Consistent with this, knockdown of *dpy-21* by RNAi led to elevation of H4K20me1 and H4K20me3 in both wild-type and *rict-1* mutant animals (Fig. 7A-D). Knockdown of *set-1* led to reductions in H4K20me1 and H4K20me3 (Fig. 7A,B), as previously published for mutant *set-1* animals (Vielle et al., 2012). Alternatively, knockdown of *set-4*

led to the largest increase in H4K20me1 levels (Fig. 7A,C) and only a slight trend towards lower H4K20me3 levels (Fig. 7B,D).

#### DPY-21 physically interacts with SGK-1

In order to address possible mechanisms of regulation of the DCC by the TORC2 pathway, we tested whether DPY-21 protein could physically associate with SGK-1. DPY-21 protein carries two potential phosphorylation sites for the TORC2 pathway kinase SGK-1, and we reasoned that the two proteins might associate. We found that purified C-terminal DPY-21 fused to glutathione-S-transferase (GST) was able to associate with and pull down SGK-1 tagged with GFP from whole-worm extract (Fig. 7E). The interaction was reproducible and specific, as free GFP did not associate with DPY-21-GST and SGK-1-GFP did not associate with GST alone (Fig. 7E).

#### DISCUSSION

In the current study, we identified *dpy-21* and the dosage compensation complex (DCC) as negative regulators of development acting downstream of the TORC2/SGK-1 pathway. *dpy-21* suppressed *rict-1* developmental delay in a reverse genetic, RNAi screen of candidate SGK-1 targets. *dpy-21* has been broadly characterized in *C. elegans* as a member of the DCC, which is involved in downregulation of the hermaphroditic X chromosome by 50% in order to prevent overexpression of potentially toxic X-linked genes (Yonker and Meyer, 2003; Meyer, 2005). We find in

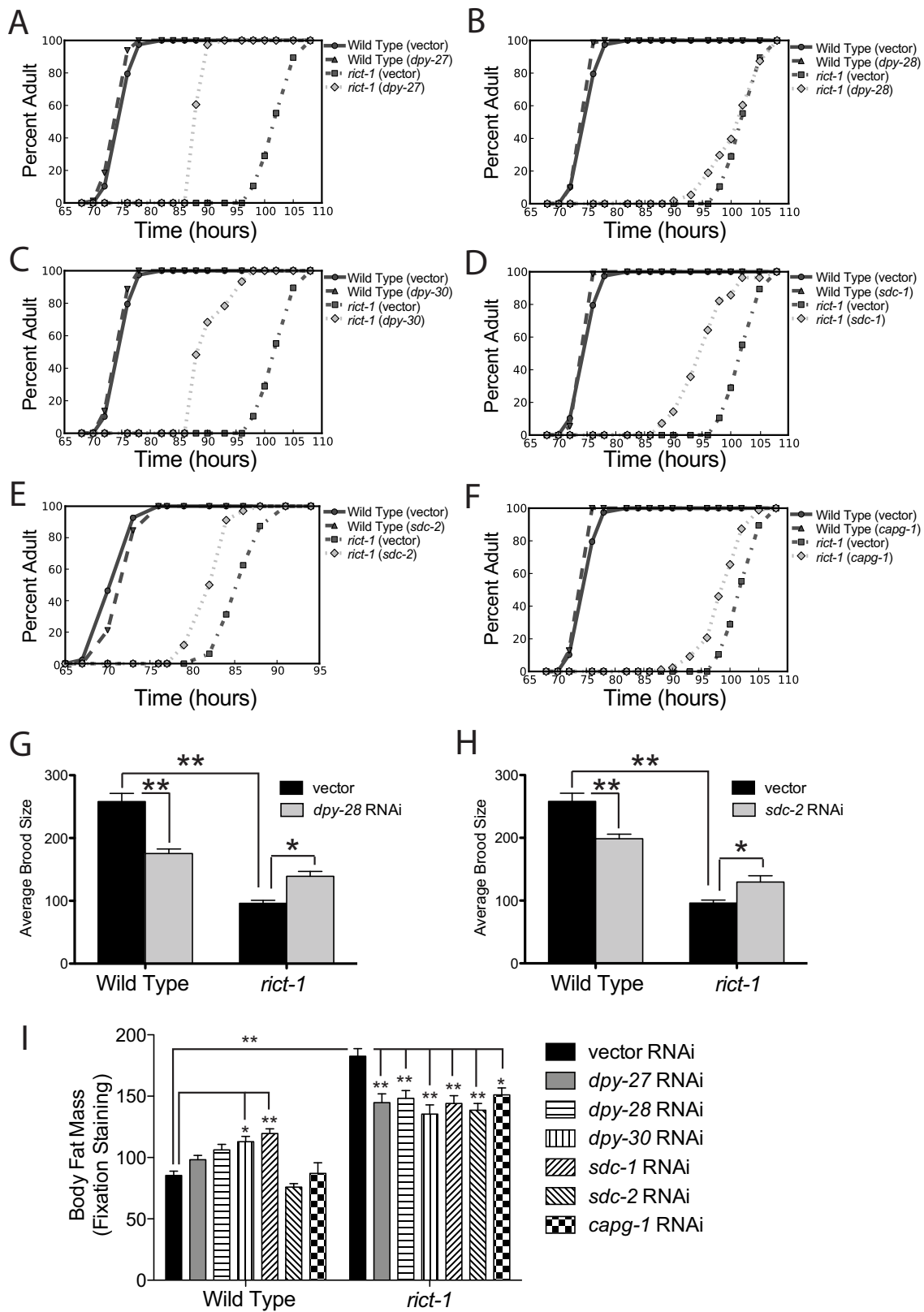


**Fig. 4. Inactivation of members of the dosage compensation complex (DCC) suppresses *rict-1* mutant developmental delay and low brood size.** (A-F) *dpy-27*, *dpy-30*, *sdc-1*, *sdc-2* and *capg-1* all showed significant suppression of *rict-1* developmental delay ( $P < 0.0001$ , log-rank test, Bonferroni-corrected vector versus DCC member RNAi for all comparisons), and had no effect on wild-type development. *dpy-28* had a trend towards accelerating development but was not significant ( $P > 0.05$ ). (G,H) Brood size of *rict-1* mutants is increased significantly by RNAi of *dpy-28* and *sdc-2*. *dpy-28* and *sdc-2* reduce viable progeny in wild-type animals. (I) RNAi of DCC components significantly decreased elevated fat mass evident in *rict-1* mutants. For G-I, \* $P < 0.01$ , \*\* $P < 0.0001$ , two-way ANOVA. Error bars represent s.e.m.

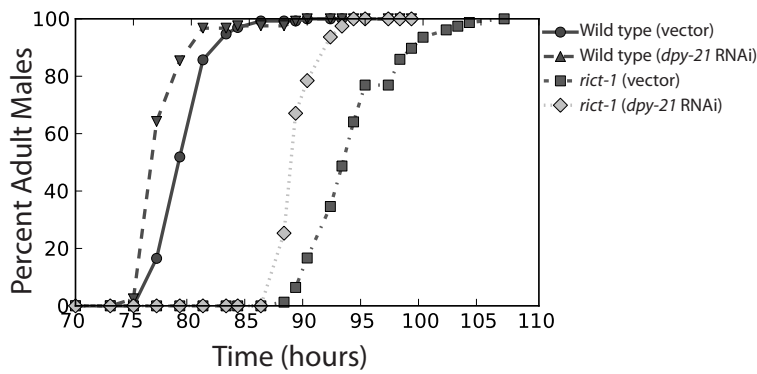


**Fig. 5. *dpy-21* RNAi acts non-canonically to suppress *rict-1* male developmental delay.** RNAi to *dpy-21* accelerates developmental rate in male *rict-1* mutants. *dpy-21* RNAi accelerated wild-type male developmental rate, but to a lesser extent than it did for *rict-1* mutants.  $P < 0.0001$  for all pairwise comparisons by log-rank test with Bonferroni correction.

this study that wild-type *dpy-21* operates downstream of the TORC2 pathway to regulate developmental rate in larval stage worms, to increase body fat and to reduce brood size. Thus, reduction in function of *dpy-21* or other members of the DCC by RNAi in *rict-1* mutants reverses the slow developmental rate, lowers body fat and raises brood size. RNAi to *dpy-21*, however, has negative effects on *rict-1* mutant body size and longevity, resulting in a

reduced lifespan and a decrease in body size. These antagonistic results suggest divergence of the TORC2 pathway upstream of DPY-21 and the DCC. The TORC2 effector kinase SGK-1 physically associates with DPY-21 protein, suggesting that physical associations between SGK-1 and the DCC are responsible for regulating its activity. We further show that the DCC is likely to be hyperactive in *rict-1* mutants, and is associated with decreased

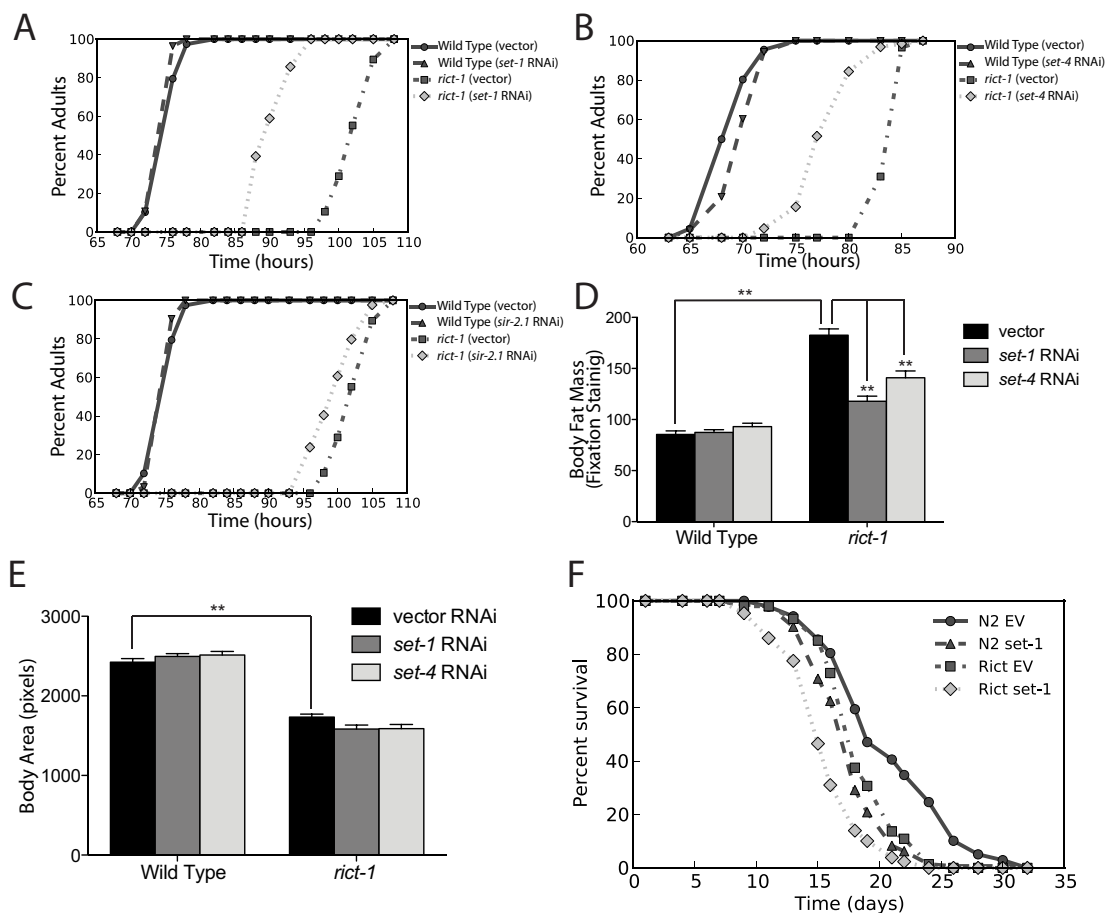


**Fig. 6. RNAi to the DCC effectors histone 4 lysine 20 (H4K20) monomethyltransferase *set-1* and di/trimethyltransferase *set-4*, suppresses *rict-1* developmental delay.** (A) RNAi to *set-1*, the H4K20 monomethyltransferase, suppresses *rict-1* developmental delay to an equivalent or greater extent than *dpy-21* RNAi.  $P < 0.0001$  by log-rank test, Bonferroni corrected for all comparisons except wild type(vector) versus wild type(*set-1* RNAi). (B) RNAi to *set-4*, the H4K20 di- and tri-methyltransferase, also increased developmental rate in *rict-1* mutants [ $P < 0.0001$ , *rict-1*(vector) versus *rict-1*(*set-4* RNAi) by log-rank test, Bonferroni corrected]. (C) RNAi to *sir-2.1* had a small but significant accelerating effect on *rict-1* developmental rate [ $P < 0.002$  by log-rank test, Bonferroni corrected for *rict-1*(vector) versus *rict-1*(*sir-2.1* RNAi)]. (D) RNAi to *set-1* and *set-4* significantly decreased fat mass in *rict-1* mutants but not in wild-type animals. (E) Like RNAi to *dpy-21* and DCC components, RNAi to *set-1* and *set-4* did not rescue small body size evident in *rict-1* mutants. For D,E,  $**P < 0.0001$ , two-way ANOVA. (F) Similar to *dpy-21*, RNAi of *set-1* did not have reproducible effects on suppressing shortened lifespan in *rict-1* mutants.

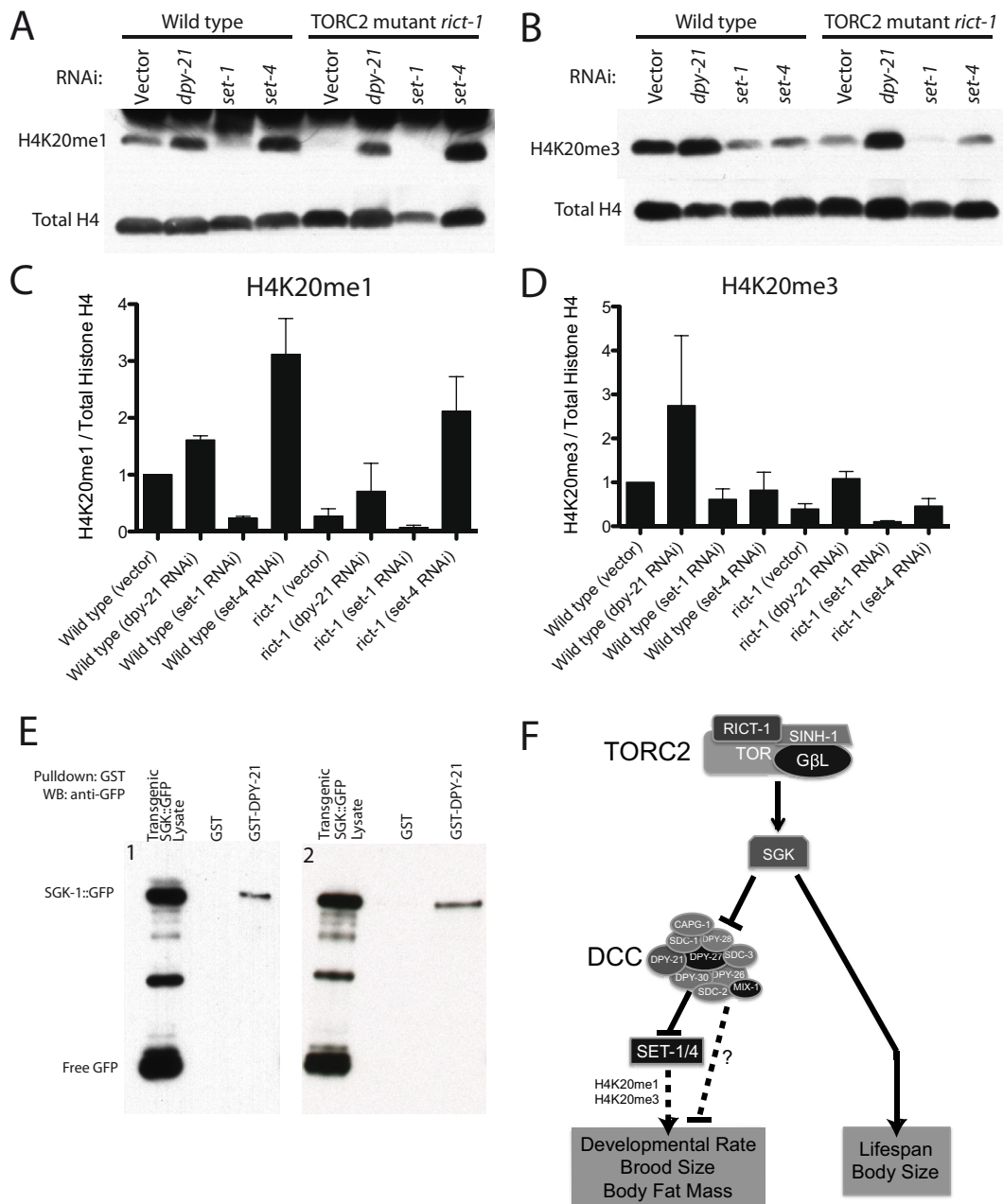


**Fig. 7. Reduced H4K20 methylation in TORC2 pathway mutant *rict-1* and physical association of DPY-21 with SGK-1.** (A,C) H4K20 monomethylation is decreased in *rict-1* mutants and is increased by RNAi to *dpy-21* in both wild type and *rict-1* mutants. RNAi to *set-1* reduced H4K20me1 as expected, but RNAi to *set-4* led to the largest increase in H4K20me1 levels. (B,D) H4K20 trimethylation is also decreased in *rict-1* mutants and increased by knockdown of *dpy-21*. RNAi to *set-1* and *set-4* led to decreased levels of H4K20me3. For C,D, data from two biological replicates were quantitated relative to total histone H4 levels. Error bars represent s.e.m. (E) A glutathione-S-transferase (GST)-tagged DPY-21 C-terminal fragment binds to SGK-1 from total worm lysate. GST-DPY-21 was expressed in *E. coli*, purified with GST resin, and incubated with total worm lysate from transgenic *C. elegans* expressing GFP-tagged SGK-1 (SGK-1::GFP). Two biological replicates are shown where DPY-21 and SGK-1 specifically interact (labeled 1 and 2). Of note, free GFP, which is also expressed by transgenic worms, does not associate with DPY-21, nor does SGK-1::GFP associate with GST alone. (F) Model of the TORC2 pathway with the DCC, SET-1 and SET-4. Under standard conditions, TORC2 functions to maintain normal developmental rate, progeny production, body fat mass, body size and lifespan. Mutation of TORC2 components *rict-1*, *sgk-1* or *sinh-1*, cause noticeable and reproducible phenotypes in each of the discussed pleiotropies. Knockdown of *dpy-21*, other members of the DCC, *set-1* or *set-4* return the body fat mass, brood size and developmental timing phenotypes of TORC2 mutants, directionally back towards that of wild-type animals. Longevity and body size are reduced equivalently by *dpy-21* knockdown in both wild-type and *rict-1* animals, suggesting that these pleiotropies are regulated by TORC2 in a DCC-independent manner.

levels of the silencing epigenetic marks H4K20me1 and H4K20me3. Our work demonstrates that the DCC acts at least partly in a non-canonical fashion to suppress TORC2 mutant

phenotypes as *dpy-21* RNAi also suppresses developmental delay of male *rict-1* mutants, in which classical dosage compensation does not occur. Finally, we can suppress *rict-1* developmental delay by

RNAi to the H4K20 monomethyltransferase *set-1* and di/trimethyltransferase *set-4*, indicating that these epigenetic marks are crucial for TORC2 mutant phenotypes.

TOR is a serine/threonine kinase that serves as a governor of cellular energetics, metabolism and growth. TOR functions as a biologically conserved core for the functionally distinct TORC1 and TORC2 complexes (Helliwell et al., 1994; Bhaskar and Hay, 2007). The TORC2/Rictor pathway has been implicated in not only cellular structure and dynamics but also energy metabolism, feeding behavior, growth, reproduction, lifespan and numerous disease states (Jacinto et al., 2004; Sarbassov et al., 2005; Bhaskar and Hay, 2007; Guertin and Sabatini, 2007; Guertin et al., 2009; Jones et al., 2009; Soukas et al., 2009). By identifying DPY-21 and the DCC as downstream effectors of TORC2, we add a new dimension to our understanding of biological outputs of TORC2.

In mammals, three AGC family kinase targets of mTORC2, SGK, AKT (protein kinase B) and protein kinase C $\alpha$  are subject to activation via TORC2-mediated phosphorylation on a conserved Ser/Thr residue within a C-terminal hydrophobic motif (HM) (Sarbassov et al., 2005; Garcia-Martinez and Alessi, 2008; Ikenoue et al., 2008). In *C. elegans*, the only known targets of SGK-1 and AKT-1 are the FoxO transcription factor DAF-16 and the stress responsive ortholog of the mammalian NRF1/2/3, SKN-1 (Paradis and Ruvkun, 1998; Brunet et al., 2001; Hertweck et al., 2004; Greer and Brunet, 2008; Tullet et al., 2008). We previously found the TORC2 *C. elegans* ortholog of Rictor, RICT-1, acts through SGK-1 to regulate reproduction, growth, feeding behavior and lifespan, and through AKT and SGK-1 to regulate fat metabolism (Soukas et al., 2009). Here, we report similarly that mutations in *sinh-1*, the *C. elegans* ortholog of Sin1 (*S. pombe* stress activated protein kinase interactor), a conserved member of TORC2 signaling pathway, led to comparable pleiotropies to *rict-1* and *sgk-1* mutant animals.

Dosage compensation (DC) is an evolutionarily conserved mechanism between mammals, flies and invertebrates for balancing sex chromosome expression between genders (Lyon, 1961; Meyer and Casson, 1986). In *C. elegans*, five proteins are involved in the core DCC, which is structurally similar to the condensin I complex: DPY-26, DPY-27, DPY-28, MIX-1 and CAPG-1 (Csankovszki et al., 2004; Meyer, 2005). The additional five associated members are SDC-1, SDC-2, SDC-3, DPY-30 and DPY-21 (Hodgkin, 1987; Hsu and Meyer, 1994; Lieb et al., 1996; Yonker and Meyer, 2003). In this work, we show that DPY-21 is most likely to be working via its role in the DCC as RNAi directed towards each DCC member tested had suppressive effects on *rict-1* phenotypes. These data comprehensively suggest that reduced function of the DCC results in beneficial effects specifically in TORC2 animals whereas wild-type animals experience minor or unfavorable effects, such as reduced progeny production.

Our results show that *dpy-21* and the DCC regulate development and metabolism downstream of TORC2 and SGK-1. RNAi of *dpy-21* in *rict-1* and *sinh-1* single mutants and in the *rict-1;sgk-1* double mutant resulted in suppression of slow developmental rate. This suggests that DPY-21 functions specifically in the TORC2 pathway downstream of *sgk-1* by virtue of its suppression of developmental phenotypes associated with mutants in TORC2, *rict-1*, *sinh-1* and *sgk-1*.

The finding that the DCC component DPY-21 physically associates with SGK-1 proteins suggests a mode of regulation of the DCC by the TORC2 pathway. We originally identified *dpy-21* by virtue of its peptide sequence, which encodes two potential SGK phosphorylation sites. The DPY-21 and SGK-1 physical interaction supports the idea that SGK-1, and therefore TORC2, directly regulate the DCC, and

may do so by phosphorylation of DPY-21. However, this conclusion requires further testing to determine the tissue and mechanism of action of the DCC in regulating TORC2 phenotypes.

Our data suggest that the DCC is negatively regulated in wild-type animals by normal activity of TORC2/SGK-1 signaling. We provide evidence that RNAi directed to *dpy-21* decreased DCC activity post-embryonically, resulting in increased levels of H4K20me1 and H4K20me3. In *rict-1* mutants, alternatively, we noted a decrease in mono- and tri-methylation of histone 4 lysine 20 (H4K20), epigenetic marks previously associated with DCC activity (Vielle et al., 2012; Wells et al., 2012). However, unlike previous studies, our data indicate that DCC activity is negatively associated with overall levels of H4K20me1 and H4K20me3. Thus, our data suggest that DCC activity is increased in TORC2 mutants, leading to lowered H4K20 methylation, growth delay, small body size, elevated fat mass and reduced brood size. It remains an open question as to how DCC activity is normally suppressed by TORC2, and what role this plays in development, although our data indicate that direct regulation by SGK-1 is a possibility. We speculate that TORC2 must modulate the DCC activity to allow for normal developmental rate while maintaining normal reproduction and metabolism (Fig. 7F). Thus, we build on the model of complex TORC2 biology in which this pathway serves as a novel descending input into the DCC linking metabolism and development to the chromatin state of *C. elegans*.

*C. elegans* TORC2 mutants have reduced life expectancy compared with wild-type animals (Fig. 2A) (Soukas et al., 2009). Lifespan analysis of wild-type and *rict-1* animals when treated with control or *dpy-21* RNAi indicates that loss of DCC functionality leads to a truncated lifespan in both backgrounds. Similarly, body size is also negatively impacted by *dpy-21* RNAi in both wild-type and *rict-1* animals. Thus, *dpy-21* knockdown results in separable phenotypes with both beneficial and detrimental outcomes. The collective data indicate that *dpy-21* acts downstream of TORC2 with regard to only certain pleiotropies (Fig. 7F). This suggests that signals from TORC2 are complex, and are not regulated by a single pathway process, but rather multiple signaling outputs. We conclude that the DCC is one of these novel outputs.

*dpy-21* and the DCC act in a non-canonical manner to suppress developmental rate downstream of TORC2. Because dosage compensation, as described in hermaphrodites, does not occur in males (Csankovszki et al., 2004), we expected *dpy-21* RNAi to have little effect on developmental timing in *rict-1* males. Surprisingly, developmental delay of *rict-1* male animals was suppressed, albeit to a lesser extent than in hermaphrodites. This indicates that at least part of the role of *dpy-21* in the TORC2 pathway must be via a novel function outside of its canonical role in X chromosomal dosage compensation. How this is mediated and to what extent regulation of X chromosomal gene expression or autosomal gene expression is involved remains to be demonstrated.

Our work shows that TORC2 mutants have reduced H4K20me1, an epigenetic mark associated with the DCC and with increased gene silencing (Vielle et al., 2012). Chromatin modification through epigenetic marks, such as histone acetylation and methylation, is a conserved, dynamic process, which alters the physical structure of the DNA and can affect other cellular processes such as transcription (Grant, 2001). In the fission yeast *S. pombe*, TORC2 signaling mutations mimic chromatin structural mutants by increasing expression from regions typically existing as heterochromatic and through underpacking of the chromatin, resulting in increased sensitivity to DNA damage and other stressors (Schonbrun et al., 2009). The epigenetic mark most associated with *C. elegans* dosage

compensation complex is the transcriptional inhibiting monomethylation of lysine 20 of histone H4 of the X chromosome in the hermaphroditic worm (Vielle et al., 2012; Wells et al., 2012). This modification is controlled through H4K20 methyltransferases SET-1 (monomethyltransferase) and SET-4 (di- and trimethyltransferase). The DCC also mediates H4K16 deacetylation on the X chromosome where SET-1, SET-4 and the Sir-2.1 histone deacetylase play regulatory roles (Wells et al., 2012).

RNAi directed toward *set-1* and *set-4* histone methyltransferases and *sir-2.1* histone deacetylase revealed that RNAi of each suppressed the slow developmental rate of *rict-1* mutants. This indicates that *rict-1* pleiotropies might in part be due to altered methylation at H4K20. This concept is further supported by western blot analysis revealing that *rict-1* animals show reduced levels of H4K20me1 and H4K20me3. However, it is clearly not simple decreases in H4K20me1 and H4K20me3 that are solely responsible for TORC2 mutant phenotypes. First, suppression of most TORC2 phenotypes studied was partial with knockdown of DCC components, along with *set-1* and *set-4*. Second, we found that *rict-1* mutants have a lower level of H4K20me1 and H4K20me3, and that this was reversed by knockdown of *dpy-21*. This suggests that post-embryonically the overactive DCC in TORC2 mutants suppresses SET-1 and SET-4, not activates them. Why then would knockdown of *set-1* and *set-4*, if their activities are already reduced in TORC2 mutants, suppress TORC2 phenotypes? It is possible that TORC2 phenotypes are due predominantly to global reduction of H4K20me1, as the levels of this mark are decreased in *rict-1* mutants and increased by *dpy-21* knockdown and *set-4* knockdown. However, because knockdown of *set-1* can also suppress TORC2 mutant phenotypes and this is associated with decreased H4K20me1, it is likely that it is not an overall level of H4K20 methylation that regulates metabolism, but rather the balance of H4K20me1 and H4K20me3 at specific promoters. Future studies of the localization of H4K20me1 and H4K20me3 in TORC2 mutants will be necessary to illuminate the specific mechanisms by which these marks act to mediate metabolic defects in TORC2 mutants.

DPY-21 and the DCC are emerging as powerful, conserved regulators of developmental and metabolic regulatory pathways. *dpy-21* also modulates development through negative regulation of the insulin signaling pathway (Dumas et al., 2013). Unlike in TORC2 signaling, the findings of K. Dumas and P. Hu show that *dpy-21* acts in its canonical role in dosage compensation as male dauer diapause entry was not affected. These observations, although probably disparate mechanistically, suggest that, either via its canonical role in dosage compensation or in a non-canonical role in TORC2 signaling, the DCC and DPY-21 are conserved regulators of growth, development and metabolism.

Further studies into the genetic mechanisms of chromatin modification in TORC2 mutants will undoubtedly offer exciting new avenues of research with the ultimate aim of understanding the role of TORC2 in the pathogenesis of disease states such as type 2 diabetes and cancer. Cellular control of transcription requires a complex series of post-translational events in order to maintain homeostatic levels of transcripts. Identification of DPY-21 and the DCC as novel regulators and signaling components of the TORC2 pathway helps to shed a new light not only on its genetic function but also the role of TORC2 in epigenetic regulation.

#### Acknowledgements

We are grateful to K. Dumas and P. Hu for sharing their results on *dpy-21*. We thank J. Avruch, E. Pino and M. Runcie for discussions and for reading the manuscript. Thanks to M. Kacergis for technical support in all aspects of the project.

#### Funding

This work was supported by a New Scholar in Aging Award from the Ellison Medical Foundation [A.S.]; a National Institutes of Health (NIH) Career Development Award [K08DK087941 to A.S.]; and the Charles H. Hood Foundation Child Health Research Award [A.S.]. Some *C. elegans* strains were provided by the *Caenorhabditis* Genetics Center, which is funded by NIH Office of Research Infrastructure Programs [P40 OD010440]. Deposited in PMC for release after 12 months.

#### Competing interests statement

The authors declare no competing financial interests.

#### Author contributions

C.M.W., L.W. and A.A.S. conceived and designed the experiments; C.M.W., L.W., D.D. and A.A.S. performed the experiments. C.M.W. and A.A.S. analyzed the data and wrote the manuscript.

#### Supplementary material

Supplementary material available online at <http://dev.biologists.org/lookup/suppl/doi:10.1242/dev.094292/-/DC1>

#### References

- Alessi, D. R., Pearce, L. R. and García-Martínez, J. M. (2009). New insights into mTOR signaling: mTORC2 and beyond. *Sci. Signal.* **2**, pe27.
- Aronova, S., Wedaman, K., Aronov, P. A., Fontes, K., Ramos, K., Hammock, B. D. and Powers, T. (2008). Regulation of ceramide biosynthesis by TOR complex 2. *Cell Metab.* **7**, 148-158.
- Bhaskar, P. T. and Hay, N. (2007). The two TORCs and Akt. *Dev. Cell* **12**, 487-502.
- Bodenmiller, B., Campbell, D., Gerrits, B., Lam, H., Jovanovic, M., Picotti, P., Schlapbach, R. and Aebersold, R. (2008). PhosphoPep – a database of protein phosphorylation sites in model organisms. *Nat. Biotechnol.* **26**, 1339-1340.
- Brunet, A., Park, J., Tran, H., Hu, L. S., Hemmings, B. A. and Greenberg, M. E. (2001). Protein kinase SGK mediates survival signals by phosphorylating the forkhead transcription factor FKHRL1 (FOXO3a). *Mol. Cell. Biol.* **21**, 952-965.
- Chuang, P. T., Albertson, D. G. and Meyer, B. J. (1994). DPY-27: a chromosome condensation protein homolog that regulates *C. elegans* dosage compensation through association with the X chromosome. *Cell* **79**, 459-474.
- Csankovszki, G., McDonel, P. and Meyer, B. J. (2004). Recruitment and spreading of the *C. elegans* dosage compensation complex along X chromosomes. *Science* **303**, 1182-1185.
- Dumas, K. J., Delaney, C. E., Flibotte, S., Moerman, D. G., Csankovszki, G. and Hu, P. J. (2013). Unexpected role for dosage compensation in the control of dauer arrest, insulin-like signaling, and FoxO transcription factor activity in *Caenorhabditis elegans*. *Genetics* **194**, 619-629.
- García-Martínez, J. M. and Alessi, D. R. (2008). mTOR complex 2 (mTORC2) controls hydrophobic motif phosphorylation and activation of serum- and glucocorticoid-induced protein kinase 1 (SGK1). *Biochem. J.* **416**, 375-385.
- Gelbart, M. E. and Kuroda, M. I. (2009). *Drosophila* dosage compensation: a complex voyage to the X chromosome. *Development* **136**, 1399-1410.
- Grant, P. A. (2001). A tale of histone modifications. *Genome Biol.* **2**, reviews0003-reviews00036.
- Greer, E. L. and Brunet, A. (2008). FOXO transcription factors in ageing and cancer. *Acta Physiol. (Oxf.)* **192**, 19-28.
- Guertin, D. A. and Sabatini, D. M. (2007). Defining the role of mTOR in cancer. *Cancer Cell* **12**, 9-22.
- Guertin, D. A., Stevens, D. M., Saitoh, M., Kinkel, S., Crosby, K., Sheen, J. H., Mullholland, D. J., Magnuson, M. A., Wu, H. and Sabatini, D. M. (2009). mTOR complex 2 is required for the development of prostate cancer induced by Pten loss in mice. *Cancer Cell* **15**, 148-159.
- Hagiwara, A., Cornu, M., Cybulski, N., Polak, P., Betz, C., Trapani, F., Terracciano, L., Heim, M. H., Rüegg, M. A. and Hall, M. N. (2012). Hepatic mTORC2 activates glycolysis and lipogenesis through Akt, glucokinase, and SREBP1c. *Cell Metab.* **15**, 725-738.
- Hansen, M., Hsu, A. L., Dillin, A. and Kenyon, C. (2005). New genes tied to endocrine, metabolic, and dietary regulation of lifespan from a *Caenorhabditis elegans* genomic RNAi screen. *PLoS Genet.* **1**, 119-128.
- Helliwell, S. B., Wagner, P., Kunz, J., Deuter-Reinhard, M., Henriquez, R. and Hall, M. N. (1994). TOR1 and TOR2 are structurally and functionally similar but not identical phosphatidylinositol kinase homologues in yeast. *Mol. Biol. Cell* **5**, 105-118.
- Hertweck, M., Göbel, C. and Baumeister, R. (2004). *C. elegans* SGK-1 is the critical component in the Akt/PKB kinase complex to control stress response and life span. *Dev. Cell* **6**, 577-588.
- Hodgkin, J. (1987). Primary sex determination in the nematode *C. elegans*. *Development* **101** Suppl., 5-16.
- Hsu, D. R. and Meyer, B. J. (1994). The *dpy-30* gene encodes an essential component of the *Caenorhabditis elegans* dosage compensation machinery. *Genetics* **137**, 999-1018.

- Ikenoue, T., Inoki, K., Yang, Q., Zhou, X. and Guan, K. L. (2008). Essential function of TORC2 in PKC and Akt turn motif phosphorylation, maturation and signalling. *EMBO J.* **27**, 1919-1931.
- Jacinto, E., Loewith, R., Schmidt, A., Lin, S., Rügge, M. A., Hall, A. and Hall, M. N. (2004). Mammalian TOR complex 2 controls the actin cytoskeleton and is rapamycin insensitive. *Nat. Cell Biol.* **6**, 1122-1128.
- Jones, K. T., Greer, E. R., Pearce, D. and Ashrafi, K. (2009). Rictor/TORC2 regulates *Caenorhabditis elegans* fat storage, body size, and development through *sgk-1*. *PLoS Biol.* **7**, e60.
- Kamada, Y., Fujioka, Y., Suzuki, N. N., Inagaki, F., Wullschleger, S., Loewith, R., Hall, M. N. and Ohsumi, Y. (2005). Tor2 directly phosphorylates the AGC kinase Ypk2 to regulate actin polarization. *Mol. Cell Biol.* **25**, 7239-7248.
- Kamath, R. S. and Ahringer, J. (2003). Genome-wide RNAi screening in *Caenorhabditis elegans*. *Methods* **30**, 313-321.
- Lamming, D. W., Ye, L., Katajisto, P., Goncalves, M. D., Saitoh, M., Stevens, D. M., Davis, J. G., Salmon, A. B., Richardson, A., Ahima, R. S. et al. (2012). Rapamycin-induced insulin resistance is mediated by mTORC2 loss and uncoupled from longevity. *Science* **335**, 1638-1643.
- Lieb, J. D., Capowski, E. E., Meneely, P. and Meyer, B. J. (1996). DPY-26, a link between dosage compensation and meiotic chromosome segregation in the nematode. *Science* **274**, 1732-1736.
- Lyons, M. F. (1961). Gene action in the X-chromosome of the mouse (*Mus musculus* L.). *Nature* **190**, 372-373.
- Meyer, B. J. (2005). X-Chromosome dosage compensation. In *Wormbook*, (ed. The C. elegans Research Community). doi/10.1895/wormbook.1.101.1: <http://www.wormbook.org>.
- Meyer, B. J. and Casson, L. P. (1986). *Caenorhabditis elegans* compensates for the difference in X chromosome dosage between the sexes by regulating transcript levels. *Cell* **47**, 871-881.
- Nguyen, C. Q., Hall, D. H., Yang, Y. and Fitch, D. H. (1999). Morphogenesis of the *Caenorhabditis elegans* male tail tip. *Dev. Biol.* **207**, 86-106.
- Nishioka, K., Rice, J. C., Sarma, K., Erdjument-Bromage, H., Werner, J., Wang, Y., Chuikov, S., Valenzuela, P., Tempst, P., Steward, R. et al. (2002). PR-Set7 is a nucleosome-specific methyltransferase that modifies lysine 20 of histone H4 and is associated with silent chromatin. *Mol. Cell* **9**, 1201-1213.
- Paradis, S. and Ruvkun, G. (1998). *Caenorhabditis elegans* Akt/PKB transduces insulin receptor-like signals from AGE-1 PI3 kinase to the DAF-16 transcription factor. *Genes Dev.* **12**, 2488-2498.
- Pino, E. C., Webster, C. M., Carr, C. E. and Soukas, A. A. (2013). Biochemical and high throughput microscopic assessment of fat mass in *Caenorhabditis elegans*. *J. Vis. Exp.* **73**, e50180.
- Rice, J. C., Nishioka, K., Sarma, K., Steward, R., Reinberg, D. and Allis, C. D. (2002). Mitotic-specific methylation of histone H4 Lys 20 follows increased PR-Set7 expression and its localization to mitotic chromosomes. *Genes Dev.* **16**, 2225-2230.
- Robida-Stubbs, S., Glover-Cutter, K., Lamming, D. W., Mizunuma, M., Narasimhan, S. D., Neumann-Haefelin, E., Sabatini, D. M. and Blackwell, T. K. (2012). TOR signaling and rapamycin influence longevity by regulating SKN-1/Nrf and DAF-16/FoxO. *Cell Metab.* **15**, 713-724.
- Rohde, J. R. and Cardenas, M. E. (2003). The tor pathway regulates gene expression by linking nutrient sensing to histone acetylation. *Mol. Cell Biol.* **23**, 629-635.
- Sarbassov, D. D., Guertin, D. A., Ali, S. M. and Sabatini, D. M. (2005). Rictor/TORC2 regulates Akt/PKB by the rictor-mTOR complex. *Science* **307**, 1098-1101.
- Schonbrun, M., Laor, D., López-Maury, L., Bähler, J., Kupiec, M. and Weisman, R. (2009). TOR complex 2 controls gene silencing, telomere length maintenance, and survival under DNA-damaging conditions. *Mol. Cell Biol.* **29**, 4584-4594.
- Soukas, A. A., Kane, E. A., Carr, C. E., Melo, J. A. and Ruvkun, G. (2009). Rictor/TORC2 regulates fat metabolism, feeding, growth, and life span in *Caenorhabditis elegans*. *Genes Dev.* **23**, 496-511.
- Tsang, C. K., Bertram, P. G., Ai, W., Drenan, R. and Zheng, X. F. (2003). Chromatin-mediated regulation of nucleolar structure and RNA Pol I localization by TOR. *EMBO J.* **22**, 6045-6056.
- Tullet, J. M., Hertweck, M., An, J. H., Baker, J., Hwang, J. Y., Liu, S., Oliveira, R. P., Baumeister, R. and Blackwell, T. K. (2008). Direct inhibition of the longevity-promoting factor SKN-1 by insulin-like signaling in *C. elegans*. *Cell* **132**, 1025-1038.
- Vielle, A., Lang, J., Dong, Y., Ercan, S., Kotwaliwale, C., Rechtsteiner, A., Appert, A., Chen, Q. B., Dose, A., Egelhofer, T. et al. (2012). H4K20me1 contributes to downregulation of X-linked genes for *C. elegans* dosage compensation. *PLoS Genet.* **8**, e1002933.
- Wells, M. B., Snyder, M. J., Custer, L. M. and Csankovszki, G. (2012). *Caenorhabditis elegans* dosage compensation regulates histone H4 chromatin state on X chromosomes. *Mol. Cell Biol.* **32**, 1710-1719.
- Yonker, S. A. and Meyer, B. J. (2003). Recruitment of *C. elegans* dosage compensation proteins for gene-specific versus chromosome-wide repression. *Development* **130**, 6519-6532.
- Yuan, M., Pino, E., Wu, L., Kacergis, M. and Soukas, A. A. (2012). Identification of Akt-independent regulation of hepatic lipogenesis by mammalian target of rapamycin (mTOR) complex 2. *J. Biol. Chem.* **287**, 29579-29588.